

Simulação numérica ortotrópica não linear para monitoramento de ensaios de embutimento de madeira de acordo com a norma europeia BS EN 383 (2007)

Non-linear orthotropic numerical simulation for monitoring wood embedment tests according to BS EN 383 (2007) Standard European

Amauri da Silva Ribas Junior¹, Tayla Castilho Criado², Alexandre Jorge Duarte de Souza³, Julio Cesar Molina²

¹Universidade Estadual Paulista, Faculdade de Engenharia e Ciências, Departamento de Engenharia Mecânica, Avenida Eriberto da Cunha, 333, Guaratinguetá, SP, Brasil.

²Universidade de São Paulo, Escola de Engenharia de São Carlos, Laboratório de Madeiras e Estruturas de Madeira, Departamento de Engenharia de Estruturas, Avenida Trabalhador São Carlense, 400, São Carlos, SP, Brasil.

³Universidade Estadual Paulista, Instituto de Ciências e Engenharia, Rua Geraldo Alckmin, 519, Itapeva, SP, Brasil. e-mail: amauri.ribas@unesp.br, tayla.criado@hotmail.com, alexandre.duarte@unesp.br, julio.molina@usp.br

RESUMO

A maioria dos estudos realizados no Brasil sobre o comportamento de conexões em estruturas de madeira é de natureza experimental, com poucos utilizando análises numéricas baseadas no Método dos Elementos Finitos (FEM). Em testes de embutimento, além de determinar os valores experimentais de resistência, é crucial entender os pontos de concentração de estresse para identificar os principais modos de falha. Este estudo teve como objetivo apresentar uma estratégia de modelagem numérica para monitorar o comportamento dos espécimes em testes de embutimento de acordo com a norma BS EN 383: 2007 [1]. Para a simulação numérica, utilizou-se o software ANSYS [2], considerando vários critérios de resistência para os materiais envolvidos. Os modelos incorporaram propriedades elásticas e plásticas dos materiais, obtidas por caracterização experimental em laboratório. Foram realizados testes experimentais de embutimento em espécimes nas direções paralela e perpendicular às fibras, usando pinos metálicos de 6.72 mm de diâmetro para calibração dos resultados numéricos. A estratégia de modelagem numérica proposta permitiu a análise global dos espécimes de teste de embutimento, bem como a investigação de aspectos localizados de interesse, como concentrações de estresse, um fator difícil de quantificar em análises experimentais.

Palavras-chave: Madeira; Embutimento; Simulação numérica; ANSYS.

ABSTRACT

Most studies conducted in Brazil to analyze the behavior of connections for wooden structures have an experimental nature, and few studies consider numerical analyses based on the Finite Element Method (FEM). In embedment tests, understanding stress concentration points is crucial for identifying primary failure modes and determining the experimental strength values. The objective of this study was to present a numerical modeling strategy to monitor the behavior of test specimens in embedment tests according to BS EN 383: 2007 [1]. The ANSYS [2] software was employed for numerical modeling, considering various strength criteria for the involved materials. The models incorporated elastic and plastic properties of the materials obtained through laboratory experimental characterization. Experimental embedment tests were conducted on specimens in parallel and perpendicular directions to the fibers, using 6.72 mm diameter metal pins for numerical result calibration. The proposed numerical modeling strategy allowed for the global analysis of embedment test specimens and the examination of localized aspects of interest, such as stress concentrations, a factor challenging to quantify in experimental analyses.

Keywords: wood; embedment; stresses; numerical simulation; ANSYS.

Corresponding Author: Tayla Castilho Criado Received on 18/08/2024 Accepted on 03/10/2024



1. INTRODUCTION

For the development of timber structures, understanding the behavior of connections between their elements is crucial [3, 4]. The highest stresses are concentrated in the connection regions, considered fundamental points for the structure's safety. In the design of pin connections, two possible forms of failure are considered: the bending of the metal pin and the embedment of the pin in wood [5]. These two failure modes can result in different types of failures, which are listed in the Brazilian standard ABNT NBR 7190-1 [6], depending on the connected elements (wood-to-wood or wood-to-steel plates) and the type of joint (single or double shear). Embedment is characterized by localized crushing or splitting that occurs in wood due to compression stresses originating from the contact of the metal pin with the wood, and this phenomenon is more commonly observed in connections [7].

The embedding behavior of solid timber has been studied by several researchers, and empirical equations to determine the due strength have been adopted by normative documents. It is noted that the embedding strength is influenced by several factors [8]. Most works in the literature regarding determining wood embedment strength are experimental [5, 9–11]. Furthermore, these models generally seek to restrict the behavior of structures to linearly elastic limits rather than considering true failure criteria for materials, thus yielding overly conservative responses [12–15].

The structures analyzed this way can withstand much higher loads than those considered during design [16]. However, the stresses and deformations generated by external loads often exceed the elastic limits of materials, and therefore, the structural response of materials should not be studied as linearly elastic. The results obtained from the linear analysis are valid if plastic deformations are small and material failure occurs for loads approaching ultimate values. It can also be stated that the geometry of structural elements, especially in connection regions, can elevate stress states to maximum levels, leading to material failure under service loads. For these reasons, the use of numerical models that allow for a more accurate determination of the proper structural behavior of materials, especially in connection regions, is of fundamental importance.

Among the existing tools for numerical analysis, some specific commercial software stands out, such as ANSYS, ABAQUS, and ADYNA, among others. These software packages are based on the Finite Element Method (FEM), and specifically, ANSYS [2] uses the Hill strength criterion as a failure criterion, which allows for the numerical reproduction of the behavior of structural elements and even entire structures, avoiding costs associated with experimental testing [15, 17]. Numerical simulation enables a detailed analysis of aspects of interest, such as stress concentrations in regions close to the most solicited areas of the analyzed element, which may not be observed in experimental tests [18, 19].

The objective of this study was to present numerical simulation strategies to represent the behavior of wooden test specimens with steel pins of diameter 6.72 mm in embedment tests, in both parallel and perpendicular directions to the wood fibers, following BS EN 383: 2007 [1]. The method outlined in BS EN 383:2007 [1] is identical to the one currently presented in ABNT NBR 7190-3 [20]. This was achieved through non-linear computational models incorporating orthotropy. The results of this research were used as a parameter for the adoption of the Brazilian test method ABNT NBR 7190-3 [20].

2. MATERIALS AND METHODS

2.1. Materials used

Australian Cedarwood (*Toona ciliata*), classified as C20, was employed for the experimental embedment tests, utilizing nails with a diameter of 6.72 mm.

2.2. Equipment used

The mechanical tests were conducted using the EMIC universal testing machine, which has a capacity of 300 kN and a specially designed metallic support device for the pin. Displacements in the embedment tests were quantified using an LVDT-type displacement transducer (Figure 1).

2.3. Experimental method

Initially, cedarwood was characterized to obtain its main physical and mechanical properties (elastic and plastic) based on ABNT NBR 7190-3: 2022 [20]. The specimen geometry and embedment test procedures followed the methodology of the European standard BS EN 383: 2007 [1], which is the same model as those adopted by the Brazilian method ABNT NBR 7190-3: 2022 [20]. The comprehensive study presented in this research considered a total of 216 embedment tests.



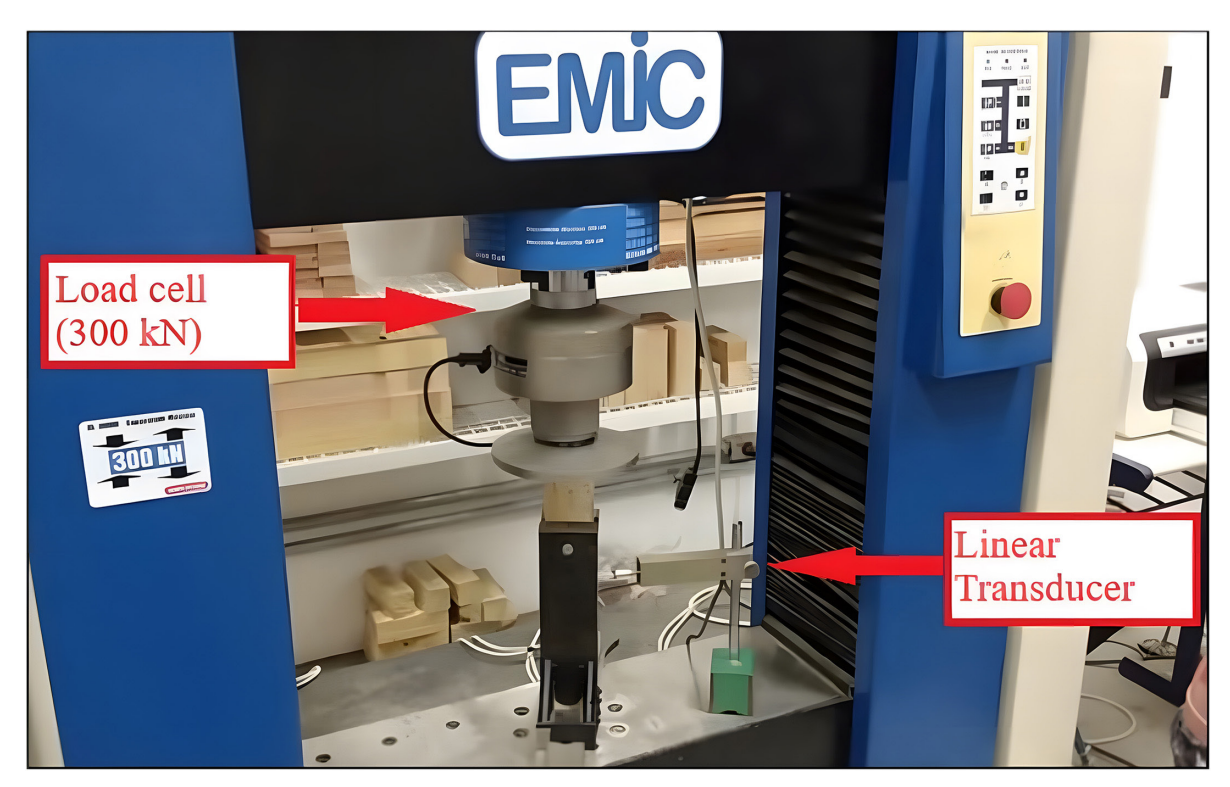


Figure 1: Scheme of the embedment test on the EMIC universal testing machine. Source: The Authors.

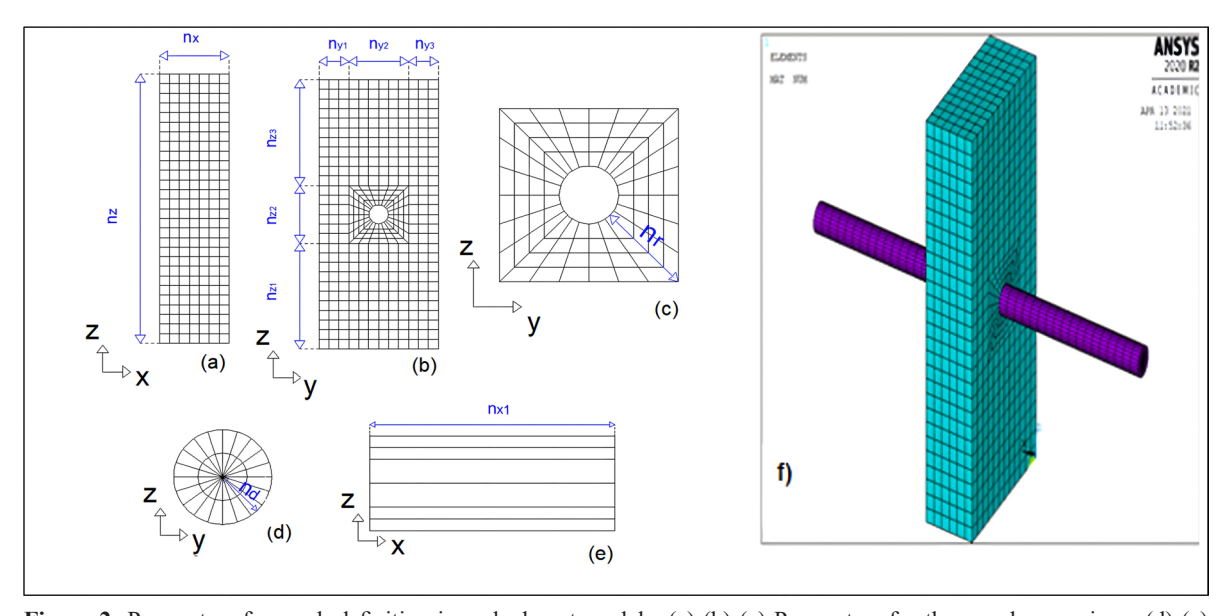


Figure 2: Parameters for mesh definition in embedment models: (a) (b) (c) Parameters for the wooden specimen (d) (e) Parameters for the metal pin (f) Finite element mesh in ANSYS (2020). Source: The Authors.

2.4. Numerical method

The ANSYS (2020), version 20, software was employed to generate numerical models of the embedment test specimens, experimentally tested in parallel and perpendicular directions to the wood fibers. Two types of materials were considered: the prismatic wooden specimen and the metal pin. The construction of the models incorporated the elastic and plastic properties of the materials.

Solid45, available in the internal library of ANSYS (2020), was employed to discretize the wooden specimen and the metal connector. This element was chosen for its representativeness in simulating the behavior. The Solid45 element (Figure 2) is a hexahedral element with eight nodes and three degrees of freedom per node (translations along the x, y, and z axes) and enables the consideration of important effects such as plasticity and orthotropy for the involved materials.

Table 1: Mesh fibers. Source:			an standard	test specimen	model in bo	th parallel ar	nd perpendic	ular directi	ons to the
MESH	N (1)	N (2)	N (3)	N (4)	N (5)	N (6)	N (7)	Nr ⁽⁸⁾	N (9)

MESH	N _x ⁽¹⁾	N _{x,1} ⁽²⁾	N _{y,1} ⁽³⁾	$N_{y,2}^{(4)}$	N _{z,1} ⁽⁵⁾	N _{z,2} ⁽⁶⁾	N _{z,3} ⁽⁷⁾	Nr ⁽⁸⁾	N _d ⁽⁹⁾
m1	4	28	2	6	8	6	8	3	1
m2	5	35	3	6	9	6	9	3	2
m3	6	42	3	6	11	6	11	4	3
m4	6	42	3	6	15	6	15	4	3

Notes: ${}^{(1)}N_x$ = the number of elements in the thickness direction of the wooden specimen; ${}^{(2)}N_{x,1}$ = the number of elements in the length direction of the metal connector; ${}^{(3)}N_{y,1}$ = the number of elements in the width direction of the wooden specimen; ${}^{(4)}N_{y,2}$ = the number of elements in the width direction of the wooden specimen in the height direction of the wooden specimen in the upper region of the test specimen; ${}^{(6)}N_{z,2}$ = the number of elements in the height direction of the wooden specimen in the region around the hole; ${}^{(7)}N_{z,3}$ = the number of elements in the height direction of the wooden specimen in the lower region of the test specimen; ${}^{(8)}N_r$ = the number of elements in the region around the hole of the wooden specimen and in the direction of the radius of the metal connector; ${}^{(9)}N_d$ = number of elements in the thickness or radius direction of the metal connector.

The adopted strength criterion for steel was the von Mises criterion for isotropic materials. For wood, the Hill strength criterion was used, considering orthotropy and plasticity for the three orthogonal directions of the wood. The behaviors of wood in tension and compression were assumed to be equal.

2.5. Mesh definition

The finite element meshes were generated and discretized within ANSYS (2020). The wood and the metal connector were generated separately; however, in the regions of the test specimen holes, the mesh discretization of the pin and wood considered coincident nodes at the contact interface. According to the European standard, the geometries of the test specimens in the parallel and perpendicular directions to the fibers were different, so it was necessary to develop two numerical models. Model 1 corresponds to the embedment test specimen model in the parallel direction to the fibers, and Model 2 corresponds to the embedment test specimen model in the perpendicular direction to the fibers.

The mesh refinement in the x, y, and z directions was defined by nine main parameters, determining the number of divisions made in each direction of interest for the test specimen. Figure 2 presents these parameters used in creating the test specimen model according to the European standard for the direction parallel to the wood fibers. This mesh construction and refinement strategy was also applied to Model 2 for the direction perpendicular to the fibers. The mesh refinement process was carried out until the simulation results, in terms of displacements and deformations, were deemed satisfactory, as shown in Table 1.

The mesh m3 was the most refined and showed the best results, so it was chosen to construct the embedment test specimen model parallel to the fibers. Meshes m1 and m2 encountered convergence errors during the model processing, which were related to excessive displacements and deformations in the x, y, and z directions. Mesh m5 was used for the test specimen in the perpendicular direction to the fibers.

2.6. Material properties

An orthotropic behavior was assumed for wood, meaning different mechanical properties for each of the three orthogonal directions considered (longitudinal, transverse, and radial). Additionally, the Hill strength criterion associated with isotropic hardening was employed for wood. The Hill criterion is available in the ANSYS software library. It extends the von Mises criterion (maximum distortion energy criterion) to account for material anisotropy, where material failure is independent of hydrostatic stresses. The Hill criterion also considers work hardening and incorporates different yield stresses along the material's three orthogonal directions.

The constitutive model used for wood was an elastic-plastic model with bilinear curves. This model had a region with purely elastic behavior, with the rest exhibiting plastic behavior. Twenty-one constants were used for wood modeling, representing its physical and mechanical properties $(E, v, G, \sigma, E_{\tau}, \tau, \text{ and } G)$ for the three material directions (Table 2 and Table 3). The relationships between the mechanical properties of wood were assumed based on the previous work (Molina 2008).

The relationships between the elastic properties of wood were assumed as $E_x = E_y = (E_z/10)$; $G = G_{xy} = G_{xz} = G_{yz} = (E_z/20)$. For the plastic properties, the assumptions were: $\sigma_z = f_e$; $(\sigma_y/\sigma_z) = (\sigma_x/\sigma_z) = 0.19$; $\tau_{xy} = \tau_{yz} = 0.38 \cdot \sigma_z$; $\tau_{xz} = 0.038 \cdot \sigma_z$; $E_{Tx} = E_{Ty} = E_{Tz}$, where f_e is the embedment strength.

A bilinear model with isotropic hardening was adopted to represent the metal connector according to the von Mises yield criterion. Four constants, namely σ_p (yield stress), E_T (tangent modulus), ρ (density), and ν (Poisson's ratio) (Table 4), were used for modeling the metal connector.



Table 2: Admitted constants for wood in the calibration of the models (elastic parameter). Source: The Authors.

PARAMETER	VAI	UNIT	
	MODEL 1	MODEL 1	
E _x ±(10)	560	560	MPa
E _v ^{±(11)}	560	5,600	MPa
E _z ±(12)	5,600	560	MPa
v _{xy} ⁽¹³⁾	0.23	0.013	Dimensionless
v _{yz} ⁽¹⁴⁾	0.013	0.013	Dimensionless
v _{xz} ⁽¹⁵⁾	0.013	0.23	Dimensionless
G _{xy} ⁽¹⁶⁾	280	280	MPa
G _{vz} ⁽¹⁷⁾	280	280	MPa
G _{xz} ⁽¹⁸⁾	280	280	MPa
$E_{x}^{\pm(10)}$	560	560	MPa
E _v ±(11)	560	5,600	MPa
E _z ±(12)	5,600	560	MPa

Notes: $^{(10)}E_x^{\ \pm}$ = Tangential modulus of elasticity; $^{(11)}E_y^{\ \pm}$ = Radial modulus of elasticity; $^{(12)}E_z^{\ \pm}$ = Longitudinal modulus of elasticity (compression); $^{(13)}v_{xy}$ = Poisson's ratio in the xy plane; $^{(14)}v_{yz}$ = Poisson's ratio in the yz plane; $^{(15)}v_{xz}$ = Poisson's ratio in the xz plane; $^{(16)}G_{xy}$ = Transverse modulus of elasticity in the yz plane; $^{(18)}G_{xz}$ = Transverse modulus of elasticity in the xz plane.

Table 3: Admitted constants for wood in the calibration of the models (plastic parameters). Source: The Authors.

PARAMETER	VAI	UNIT	
	MODEL 1	MODEL 1	
$\sigma_{x}^{\pm(19)}$	4.37	4.37	MPa
$\sigma_{_{\mathrm{V}}}^{^{\pm(20)}}$	4.37	4.37	MPa
σ _z ±(21)	23.1	23.1	MPa
τ _{xy} ⁽²²⁾	8.74	8.74	MPa
τ _{yz} ⁽²³⁾	8.74	8.74	MPa
$ au_{xz}^{(24)}$	0.874	0.874	MPa
$E_{Tx}^{\pm(25)}$	3.43	3.43	MPa
E _{Ty} ±(26)	3.43	3.43	MPa
$E_{Tz}^{\pm(27)}$	234.33	234.33	MPa
G _{Txy} (28)	15.06	15.06	MPa
G _{Tyz} ⁽²⁹⁾	15.06	15.06	MPa
$G_{Txz}^{(30)}$	0.015	0.015	MPa

Notes: $^{(19)}\sigma_x^{\ \pm}$ = Plastic yield stress (tension and compression) in the x direction; $^{(20)}\sigma_y^{\ \pm}$ = Plastic yield stress (tension and compression) in the z direction; $^{(22)}\tau_{xy}^{\ \pm}$ = Plastic shear yield stress in the xy plane; $^{(23)}\tau_{yz}^{\ \pm}$ = Plastic shear yield stress in the xy plane; $^{(24)}\tau_{xz}^{\ \pm}$ = Plastic shear yield stress in the xz plane; $^{(25)}E_{Tx}^{\ \pm}$ = Tangent modulus (tension and compression) in the x direction; $^{(26)}E_{Ty}^{\ \pm}$ = Tangent modulus (tension and compression) in the z direction; $^{(26)}E_{Ty}^{\ \pm}$ = Tangent modulus (tension and compression) in the z direction; $^{(26)}E_{Ty}^{\ \pm}$ = Tangent shear modulus in the xy plane; $^{(29)}G_{Tyz}^{\ \pm}$ = Tangent shear modulus in the yz plane; $^{(30)}G_{Tyz}^{\ \pm}$ = Tangent shear modulus in the xz plane.

Table 4: Admitted constants for the steel of the metal connectors. Source: The Authors.

PARAMETER	VALUE	UNIT
E_{T}	6,328	MPa
σ_{p}	337	MPa
ν	0.30	Dimensionless
ρ	7.85 E-4	N/mm ³



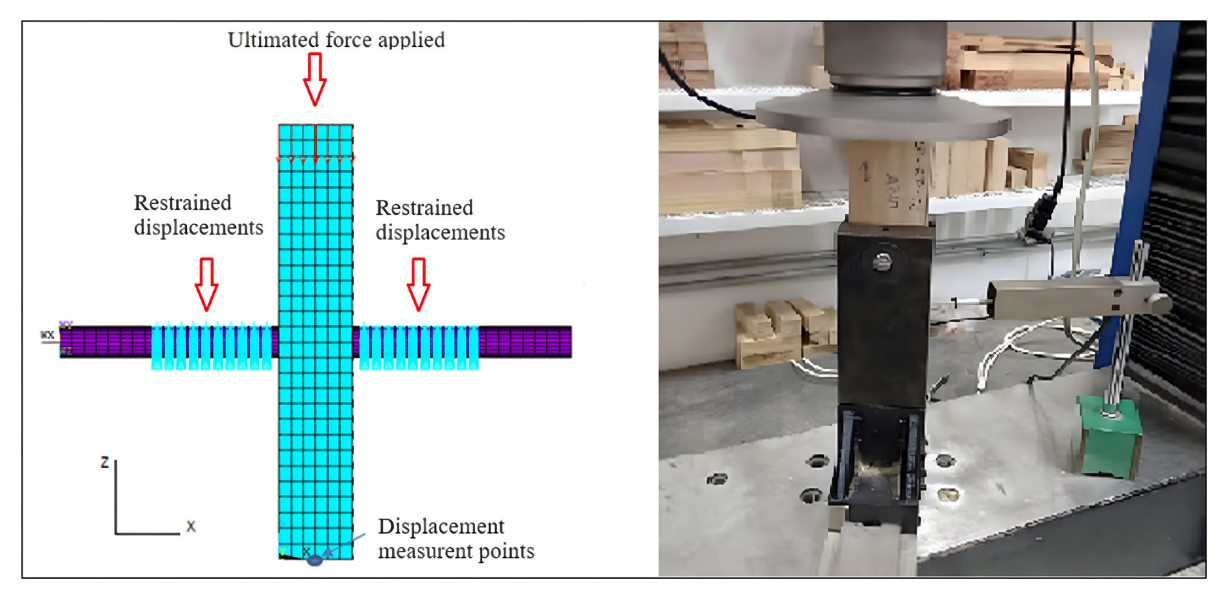


Figure 3: Constraining and loading applications for the numerical model. Source: The Authors.

2.7. Boundary conditions and loading applications

The boundary conditions and loading applications were performed to replicate the conditions of the experimental tests. For the test in the parallel direction to the fibers, the average failure force (3,064.9 N) obtained in the experimental test was applied in the z-direction, distributed across all nodes (91 nodes) on the surface of the test specimen. Thus, an applied force of 33.68 N was considered at each node. The displacements (translations) of the nodes (in the y and z directions) of the metal pin were also restricted to represent the experimental test. For the perpendicular direction to the fibers, the average failure force (2,424.20 N) was applied at the center of the test specimen (91 nodes) in the y-direction, and thus, at each node, a force of 26.24 N was considered. The displacements in the embedment tests were verified for the central bottom node of the test specimen (Figure 3).

The load increment was controlled using the ANSYS (2020) feature called "Automatic Time Stepping". This feature reduces the increment value when the predicted number of iterations exceeds the established limit in case increments of plastic deformations greater than 15% are obtained, or excessive displacements occur. The load steps were controlled using the "Time increment" option, and a convergence parameter with a tolerance of 0.001 was employed.

3. RESULTS AND DISCUSSION

3.1. Model calibration

The calibration curves of the models (Figure 4) compare the embedment force (F_e) response versus displacement (δ) of the lower reference point of the test specimen (Figure 3). It is worth noting that each point on the experimental curve represents the average of several curves obtained in the experimental tests. The numerical curves were plotted up to the point where the numerical models converged.

In general, the numerical force-displacement curves approximated the experimental curves and exhibited a linear segment followed by a non-linear segment after the onset of material yielding. In the initial segment of the numerical curve (linear part), the stiffness (characterized by the slope of the curve) was either lower or higher than the experimental stiffness, depending on the test specimen model. The second part of the curves, corresponding to the nonlinear segment, showed behaviors like the experimental curves, eventually converging for values close to the experimental failure force. Model 1 showed an average error of 10% in the linear section (from 0 to 2,000 N) and 12% in the non-linear section (from 2,000 N to 3,000 N). On the other hand, Model 2 had a higher average error, with 23% in the linear section (from 100 N to 1,500 N). and 6% in the non-linear section (from 1,500 N to 2,400 N). This difference can be attributed to a significant shift in the experimental curve at the start of measurements in Model 2, likely due to the settling of the measurement equipment.

The differences between the numerical and experimental curves arise from the complexity of modeling wood, given the presence of imperfections (distortions in fiber directions, knots, etc.). In each orthogonal direction (longitudinal, radial, and tangential), wood exhibits different mechanical properties and behaviors in tension and compression. In compression, the behavior is approximately plastic and can be approximated by an

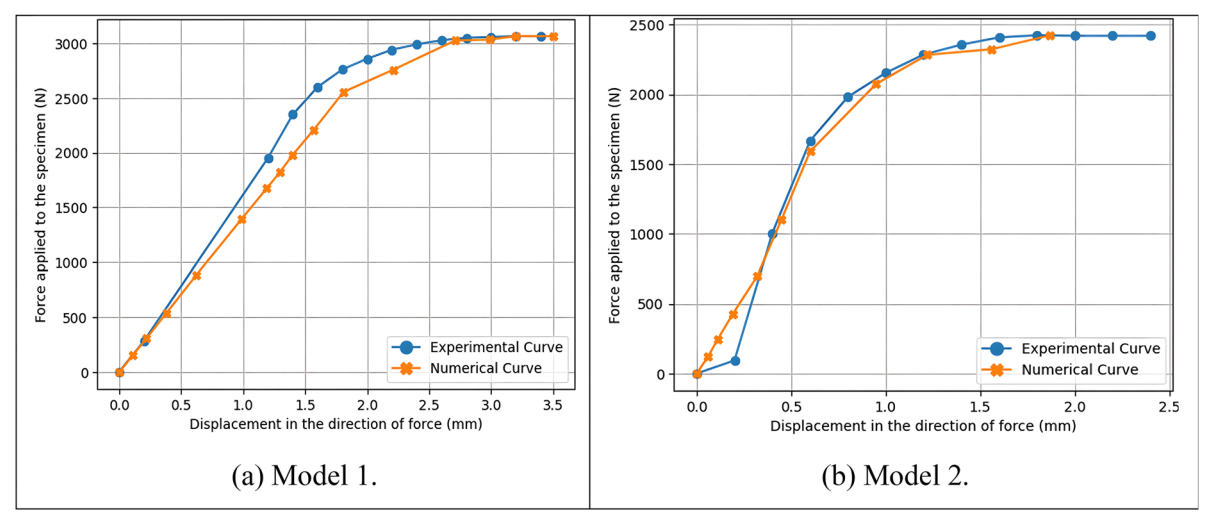


Figure 4: Calibration curves of the numerical models (a) Model 1 (parallel to the direction of the fibers) (b) Model 2 (perpendicular to the direction of the fibers). Source: The Authors.

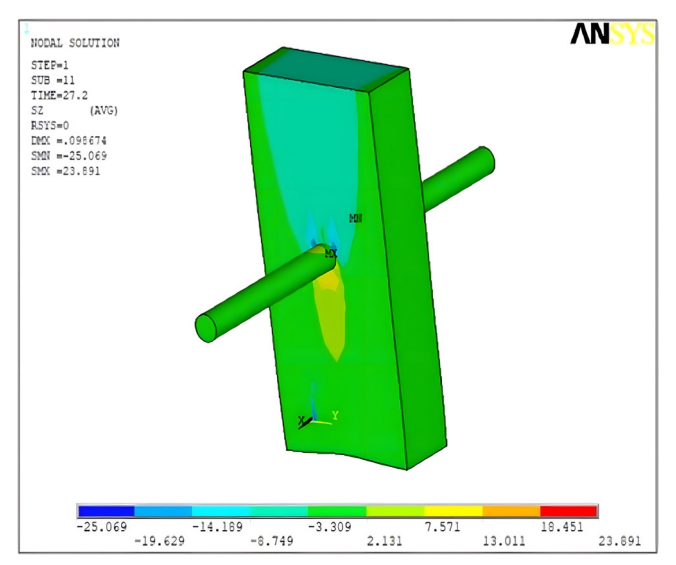


Figure 5: Stresses in MPa for Model 1 are parallel to the direction of the fibers in the z-direction. Source: The Authors.

elastic-plastic constitutive law. On the other hand, in tension, wood behaves elastic-brittle, and in this case, the elastic-plastic behavior does not truly represent the material's behavior.

It is worth mentioning that the elastic properties of wood did not significantly influence the behavior of the numerical calibration curve. However, the plastic properties had the most significant impact on the numerical force-displacement curve response, as the yield stress increased the system's strength and stiffness.

3.2. Stresses in the embedment test specimen

The computational simulation results evaluated stress levels in the evaluated test specimens, indicating compressions and damages (modes of failure) of wood in the regions of interest, as observed in the experimental tests.

3.3. Model 1

Figure 5 provides an overview of the stress results obtained for Model 1 after simulation, indicating regions of higher wood demand.

In Figure 5, the stress concentration in the regions around the hole in the central part of the test specimen was observed due to the contact of the pin with the wood. The maximum compressive stress occurred in the upper internal region of the hole and was -25.069 MPa. A maximum tensile stress of +23.891 MPa occurred in the wood region below the pin. Additionally, near the load application region (top of the wooden specimen),



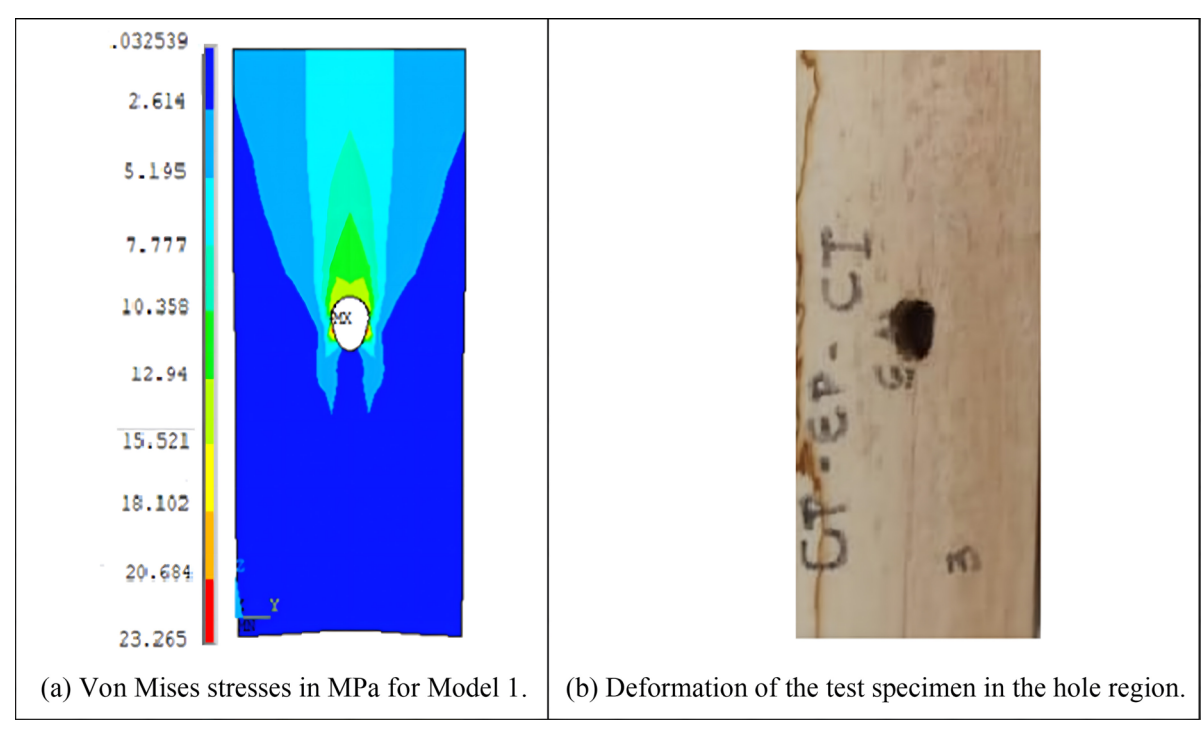


Figure 6: Comparison between numerical and experimental results (a) Numerical von Mises stress in MPa (b) Specimen after embedding test in the hole region. Source: The Authors.

the compressive stress values were approximately three times smaller than those in the contact region between the pin and the wood. Furthermore, the stress distributions in these two regions were entirely different.

Figure 6 compares the von Mises stresses obtained by numerical Model 1 with the failure mode obtained by the test specimen in the embedment experimental test.

From the previous figures, it was observed that stress concentrated in the regions around the hole in the central part of the test specimen due to the contact of the pin with the wood. There was a good approximation between the stress obtained by the numerical model and the embedment stress obtained in the experimental test. The maximum numerical stress obtained in Model 1 was 23.26 MPa, while the experimental stress was 27.20 MPa. It was also possible to observe that the stress distribution around the hole was like the deformations obtained in the test specimen during the experimental pin embedment in wood.

3.4. Model 2

Figure 7 provides an overview of the stress results obtained for Model 2 after simulation, indicating regions of higher wood demand.

The maximum numerical compressive stress normal to the wood fibers was approximately -6.711 MPa in the upper internal part of the wood hole. The compressive stress values in the load application region were approximately 2.5 times smaller than those in the contact region between the pin and the wood. In the lower part of the pin, below the hole, the maximum tensile stresses reached +5.044 MPa.

Figure 8 compares the von Mises stresses obtained by numerical Model 2 with the failure mode obtained by the test specimen in the embedment experimental test.

In Figure 8, the maximum von Mises stress obtained by numerical Model 2 was 11.08 MPa. Due to the pin's contact with the wood, stress concentrations were observed in the regions around the hole in the central part of the specimen, and stress distributions around the hole were similar to those obtained in the experimental test specimen. The results obtained in this study are consistent with previous work for a similar modeling approach [21].

The numerical modeling strategy developed for the embedment test specimens, which considered orthotropy for wood based on elastic and plastic properties and different strength criteria for the materials involved, proved to be efficient in evaluating the specimens' behavior.

The plastic properties had the most influence on the model's response. Changes in elastic properties did not result in large differences in stress results. Increases in plasticization stress increased the strength of the test specimens.

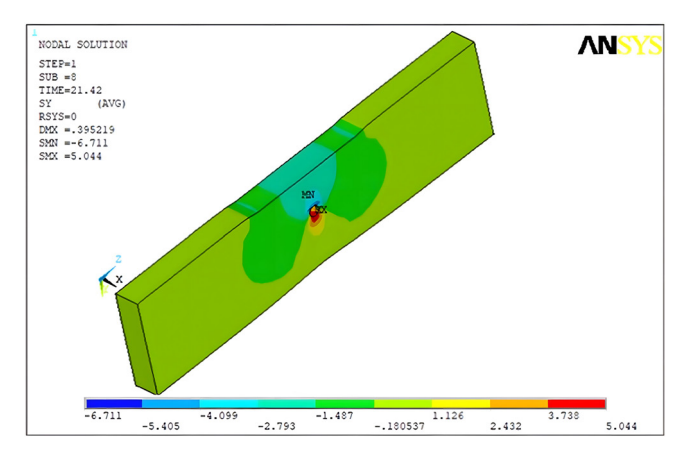


Figure 7: Stresses in MPa for Model 2 perpendicular to the fibers in the y direction with complete geometry without the metallic pin. Source: The Authors.

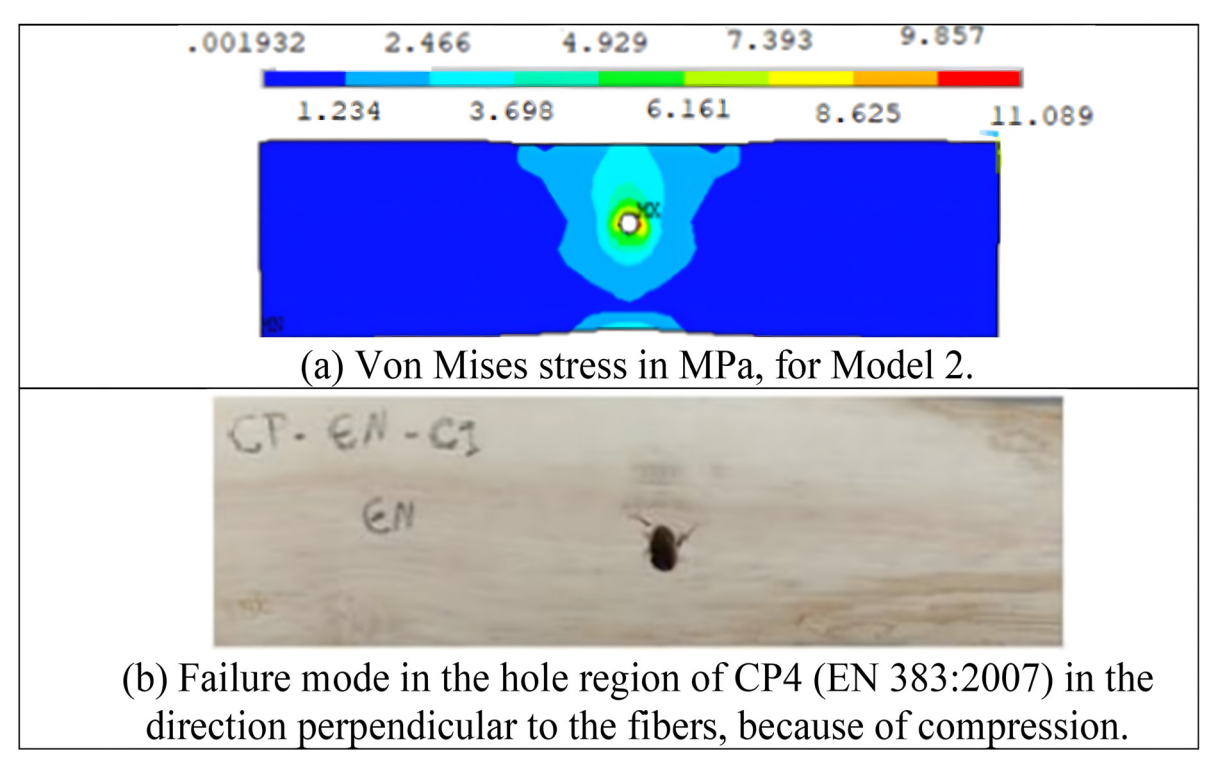


Figure 8: Stresses in MPa for model 2 perpendicular to the fibers in the y direction with complete geometry, without the metal pin. Source: The Authors.

On the other hand, as soon as the specimens' loading process begins, the elastic properties almost completely lose the influence they exert at the beginning of the behavior of the force versus displacement curve.

The proposed numerical models could simulate the mechanical behavior of the embedment test specimens in the linear elastic and nonlinear phases when the plasticization process begins. Additionally, the models allowed for the analysis of global aspects, such as the force-displacement relationship, and localized aspects, such as the verification of stresses in different regions of interest in the models.

4. CONCLUSIONS

The numerical modeling strategy developed for the embedment test specimens, which considered orthotropy for wood based on elastic and plastic properties and different strength criteria for the materials involved, proved to be efficient in evaluating the specimens' behavior.

The plastic properties had the greatest influence on the model's response. Changes in elastic properties did not result in large differences in stress results. Increases in plasticization stress increased the strength of the test specimens.



On the other hand, as soon as the specimens' loading process begins, the elastic properties almost completely lose the influence they exert at the beginning of the behavior of the force versus displacement curve.

The proposed numerical models could simulate the mechanical behavior of the embedment test specimens in the linear elastic and nonlinear phases when the plasticization process begins. Additionally, the models allowed for the analysis of global aspects, such as the force-displacement relationship, and localized aspects, such as the verification of stresses in different regions of interest in the models.

5. ACKNOWLEDGMENTS

CAPES-Coordenação de Aperfeiçoamento de Pessoal de Nível Superior.

6. BIBLIOGRAPHY

- [1] BRITISH STANDARD INSTITUTE, EN 383: Timber structures-Test methods-Determination of embedding strength and foundation values for dowel type fasteners, Brussels, BSI, 2007.
- [2] ANSYS. ANSYS version 20.0 Documentation. Canonsburg, PA: ANSYS, Inc, 2020.
- [3] MOLINA, J.C., RIBAS JUNIOR, A.S., "Resistência de embutimento em amostras padronizadas de madeira segundo as normas brasileira, europeia e americana", In: Gonçalves, F.G. (Ed.), *Engenharia Industrial Madeireira: Tecnologia, Pesquisa e Tendências, Editora Científica Digital*, Guarujá, Científica Digital, pp. 317–329, 2020. doi: http://doi.org/10.37885/201001793.
- [4] CALIL NETO, C., MOLINA, J.C., CALIL JUNIOR, C., *et al.*, "Modelagem numérica do comportamento de ligações com parafusos auto-atarraxantes em X em corpos de prova de MLC com madeiras do tipo Eucalipto urograndis", *Matéria (Rio de Janeiro)*, v. 22, n. 1, pp. e11789, 2017. doi: http://doi.org/10.1590/s1517-707620170001.0121.
- [5] ALMEIDA, D.H., DIAS, A.A., "Resistência da madeira ao embutimento perpendicular às fibras: comparação de métodos de ensaio", *Ambiente Construído*, v. 19, n. 4, pp. 175–181, Oct. 2019. doi: http://doi.org/10.1590/s1678-86212019000400349.
- [6] ASSOCIAÇÃO BRASILEIRA DE NORMAS TÉCNICAS, NBR 7190-1: Projeto de estruturas de madeira. Parte 1: Critérios de dimensionamento, Rio de Janeiro, ABNT, 2022.
- [7] MOLINA, J.C., RIBAS JUNIOR, A.S., CHRISTOFORO, A.L., "Embedding strength of Brazilian woods and recommendation for the Brazilian standard", *Proceedings of the Institution of Civil Engineers. Structures and Buildings*, v. 173, n. 12, pp. 948–955, Nov. 2020. doi: http://doi.org/10.1680/jstbu.19.00137.
- [8] MAIA, B.B., MIOTTO, J.L., GÓES, J.L.N.D., "Embedding strength of fully-threaded dowel-type fasteners in cross-laminated timber: an experimental study", *Matéria (Rio de Janeiro)*, v. 26, n. 3, pp. e13054, 2021. doi: http://doi.org/10.1590/s1517-707620210003.13054.
- [9] OLIVEIRA, M.A.M., "Ligações com pinos metálicos em estruturas de madeira", Dissertação de M.Sc., EESC/USP, São Carlos, SP, Brasil, 2001.
- [10] SANTOS, C.L., JESUS, A.M.P., MORAIS, J.J.L., "Embedment strength characterization of pine wood. Numerical study of the non-linear behaviour", *Ciência e Tecnologia dos Materiais*, v. 27, n. 1, pp. 15–26, 2015. doi: http://doi.org/10.1016/j.ctmat.2015.04.003.
- [11] TERRIN, M.V.P., GÓES, J.L.N., PLETZ, E., "Avaliação experimental da madeira ao embutimento", In: XVI EBRAMEM III CLEM, São Carlos, 2018.
- [12] ARAUJO, P.L.S., SOUZA, A.J.D., RIBAS JUNIOR, A.S., "Estudo numérico e experimental de elementos estruturais de madeira sujeitos a tração normal às fibras segundo as normas ABNT NBR 7190-3:2022 e ISO 13910:2005", *Revista Foco*, v. 16, n. 10, pp. 1–17, Nov. 2023. doi: http://doi.org/10.54751/revista-foco.v16n10-069.
- [13] KARAGIANNIS, V., MÁLAGA-CHUQUITAYPE, C., ELGHAZOULI, A.Y., "Modified foundation modelling of dowel embedment in glulam connections", *Construction & Building Materials*, v. 102, n. 2, pp. 1168–1179, Jan. 2016. doi: http://doi.org/10.1016/j.conbuildmat.2015.09.021.
- [14] SANDHAAS, C., RAVENSHORST, G.J.P., BLASS, H.J., *et al.*, "Embedment tests parallel-to-grain and ductility aspects using various wood species", *Holz als Roh- und Werkstoff*, v. 71, n. 5, pp. 599–608, Jun. 2023. doi: http://doi.org/10.1007/s00107-013-0718-z.
- [15] XU, B.H., BOUCHAÏR, A., RACHER, P., "Appropriate wood constitutive law for simulation of nonlinear behavior of timber joints", *Journal of Materials in Civil Engineering*, v. 26, n. 6, pp. 04014004, Jun. 2014. doi: http://doi.org/10.1061/(ASCE)MT.1943-5533.0000905.

- [16] MOLINA, J.C., "Strategy for numeric modelling of composite systems considering different models of rupture for the materials", *Revista Chilena de Ingenieria*, v. 17, n. 2, pp. 256–266, Aug. 2009. doi: http:// doi.org/10.4067/S0718-33052009000200014.
- [17] MOLINA, J.C., "Análise do comportamento dinâmico da ligação formada por barras de aço coladas para tabuleiros mistos de madeira e concreto para pontes", Tese de D.Sc., EESC/USP, São Carlos, SP, Brasil, 2008. doi: http://doi.org/10.11606/T.18.2008.tde-04082008-111830.
- [18] KONOPKA, D., GEBHARDT, C., KALISKE, M., "Numerical modelling of wooden structures", *Journal of Cultural Heritage*, v. 27, pp. S93–S102, Oct. 2017. doi: http://doi.org/10.1016/j.culher.2015.09.008.
- [19] NIE, Y., VALIPOUR, H.R., "Experimental and numerical study of long-term behaviour of timber-timber composite (TTC) connections", *Construction & Building Materials*, v. 304, pp. 124672, Oct. 2021. doi: http://doi.org/10.1016/j.conbuildmat.2021.124672.
- [20] ASSOCIAÇÃO BRASILEIRA DE NORMAS TÉCNICAS, NBR 7190-3: Projeto de estruturas de madeira. Parte 3: Métodos de ensaio para corpos de prova isentos de defeitos para madeiras de florestas nativas, Rio de Janeiro, ABNT, 2022.
- [21] DIAS, A.M.P.G., "Mechanical behaviour of timber-concrete joints", Tese de D.Sc., Technical University of Delft, Netherlands, 2005. doi: https://resolver.tudelft.nl/uuid:fc148f88-9ad7-4322-8dda-af121c940b62, accessed in October, 2024.